中国科学院

博士后研究报告

多像强引力透镜系统流量关系的研究

褚 哲

合作导师: 李国亮 研究员

工作完成日期: 2014 年 2 月— 2017 年 6 月

报告提交日期: 2017 年 7 月

中国科学院紫金山天文台

2017 年 7 月

Typeset by LaTeX 2ε at July 10, 2017

With package `PostDocRep` v0.1e of CTeX.ORG

多像强引力透镜系统流量关系的研究

Research on the Flux Relation for Multiple-image System in Strong Gravitational Lensing

博士后姓名 褚哲

流动站（一级学科）名称 天文学

专　业（二级学科）名称 天体物理学

研究工作起始时间 2014年2月

研究工作期满时间 2017年6月

单位名称 中国科学院紫金山天文台

报告提交日期 2017年7月

Abstract

本出站报告以强引力透镜中多像系统的流量研究为基础，着重研究了四像透镜模型中，尖角类型，折叠线类型和爱因斯坦十字类型透镜系统的流量关系。首先我们综述了5个常用的四像透镜模型，然后基于放大不变量我们分别计算了这5个透镜模型的尖角三像的放大关系，我们发现尖角放大倍数之和通常不为0，而且与透镜的参数存在着非常明显的依赖关系。基于放大不变量，我还计算了位于轴线上的尖角放大倍数之和以及尖角关系。一般认为主尖角关系要大于次尖角关系。通过我们的解析结果发现，次尖角关系也是可以大于主尖角关系的，只是这对应于极端偏离轴对称的模型，在真实的宇宙中并不多见。这些结果对将来研究多像类星体透镜系统的流量反常现象有很大的帮助作用。我们还采用数值方法研究了一些椭圆四像透镜的放大关系，经过加入迭代算法，大幅度改进了ray-tracing程序计算像的位置和放大倍数的计算精度。我们依次检验了平滑的椭圆透镜的尖角关系，折叠线关系，并分别研究了这些关系随着张角的变化。此外，我们还定义了一种新的统计量cross relation，随后我们统计了9个已经探测到的爱因斯坦十字，其中包括7个类星体，1个星系，以及1个超新星系统。我们基于不同的波段分别计算了它们的流量关系以及像的距离比。相比于尖角和折叠线构型的多像系统，我们发现爱因斯坦十字系统并不表现出明显的流量反常现象。但是对于这9个爱因斯坦十字系统，通过观测计算的结果与理论预言的cross relation存在着较大的差别，我们分别给出了一些理论上可能的解释。我们期待基于未来更精确的观测以及更完善的透镜模型将会得到比较好的一致性。除此之外，我们还把流量关系应用到FRB双峰的引力透镜机制上。我们基于FRB双峰的引力透镜机制，给出了透镜体黑洞质量以及张角的直接计算公式。然后我们通过数值的ray-tracing方法，检验了黑洞产生FRB双峰的放大倍数R与时间延迟Δt之间的对应关系，数值结果与理论符合的非常好。然后我们研究了当宇宙中存在外部剪切的情况，发现加上剪切γ可以一定概率上产生流量反转的双峰，也就是后到的峰可以比先到的峰高。我们同样采用了数值的ray-tracing去检验放大倍数R与时间延迟Δt之间关系。最后研究了当存在剪切时采用我们的公式对黑洞质量探测精确度的影响，我们发现对于$\gamma = 0.01$的剪切，对质量的影响大概只有7%左右。

Keywords: 引力透镜, 类星体, 快速射电暴

目　录

表　　格

插　　图

第一章　Introduction

强引力透镜最显著的一个特征是可以产生多像系统。多像系统的透镜体以星系居多，此外星系团也经常会产生多像系统。源天体一般为致密的类星体，也有的是星系或超新星。1979年，Walsh et al. [111]第一次观测到两个相距6角秒的天体，它们具有相同的颜色，红移和光谱。这两个天体就是类星体QSO 0957+561，这是观测到的第一个引力透镜现象。到目前为止，已经有100多个多像系统被观测到[1]，一般以两像和四像系统居多。本论文工作主要研究的就是强透镜的多像性。

在多像系统中，每个像的流量并不是独立的，每个像与其他的像之间也存在着一定的联系。这种关系我们称之为多像系统的放大关系或流量关系。强引力透镜系统的放大关系包括放大不变量，尖角关系和折叠线关系。

放大不变量（Magnification Invariant）是指对于一些特定的透镜模型，同一个点源对应的所有像的放大倍数之和是一个不变量[34, 119]，也就是$\sum_i \mu_i =$ invariant。这里的放大倍数μ是指带符号的放大倍数。很有意思的是，这个不变量几乎不依赖于透镜参数，对于不同的透镜模型有着不同大小的不变量。如上一节所示，点质量透镜的放大不变量为1，SIS透镜的不变量为2，它们都不依赖于透镜体的质量，或者说爱因斯坦半径的大小。

Dalal [34]曾对放大不变量做了系统的研究，并且给出一些透镜模型的放大不变量，如下面的表格1.1所示。Witt & Mao [119]曾对SIED透镜做了详细的研究，发现它的不变量约为2.8，也是几乎不依赖于透镜参数q的变化。

在前面所说的这些工作中，除了点透镜和SIS透镜，其他透镜很难计算对应任意点源的每个像的放大倍数。常用的方法是把透镜方程和放大倍数公式联立起来，消掉像的位置坐标等其他一些参数，得到只含有放大倍数μ的一个高次多项式。这个多项式会非常的繁琐，放大不变量就可以根据多项式两个最高次项的系数得到[34]。

尖角和折叠线关系相对于放大不变量来说，是局地的放大关系。我们知道在临界曲线上满足$\det \mathcal{A} = 0$。尖角是焦散曲线上的奇点，在临界曲线上对应于

[1] http://www.cfa.harvard.edu/castles/

表 1.1: 一些简单透镜的放大不变量[34, 35, 119]

Model	Lens potential ψ	$\sum_i \mu_i$
Point lens	$b\ln r$	1
SIS	br	2
SIEP	$b\sqrt{q^2x^2+y^2}$	2
SIQ	$br-(k/3)br\cos 2\phi$	1
Point+shear	$b\ln r+(\gamma/2)r^2\cos 2\phi$	$1/(1-\gamma^2)$
SIS+shear	$br+(\gamma/2)r^2\cos 2\phi$	$2/(1-\gamma^2)$
SIEP+shear	$b\sqrt{q^2x^2+y^2}+(\gamma/2)r^2\cos 2(\phi-\phi_\gamma)$	$2/(1-\gamma^2)$
SIED	$x\alpha_x+y\alpha_y$	≈ 2.8

其中k为四极矩的相对强度，q是椭圆透镜的轴比，γ为外部剪切。

尖角的点还满足另外一个性质，也就是雅克比矩阵在沿着临界曲线方向上的分量等于0。当一个点源在轴线上从外部穿进一个尖角时，它的一个像将会穿越临界曲线，同时在这个像的两侧增加出两个像，像的数目从一个变为三个。其中两侧的两个像的符号是相同的，它们与中间那个像的符合相反。

研究尖角奇点常用的方法是，把费马势在尖角所对应的临界曲线上展开，忽略掉高阶项，然后通过费马势的一阶导数等于0，可以得到对应尖角附近的透镜方程为

$$\beta_1 \simeq a\theta_1^3 + b\theta_1\theta_2, \tag{1.1}$$

$$\beta_2 \simeq \frac{b}{2}\theta_1^2 + c\theta_2. \tag{1.2}$$

其中a，b和c为常数。通过透镜方程可以解得，当这个点源无限地接近一个尖角的内侧时，那三个像的放大倍数均为无穷大，这时这三个像的放大倍数满足一个关系[14, 77, 102]

$$R_{\rm cusp} = \frac{\mu_{\rm A}+\mu_{\rm B}+\mu_{\rm C}}{|\mu_{\rm A}|+|\mu_{\rm B}|+|\mu_{\rm C}|} = 0, \tag{1.3}$$

其中A，B，C分别表示了这三个像，这个结果不依赖于透镜模型。有些观点认为这个公式的分子也是为0[2, 114]，在本论文的第二章我们将证明分子通常不为0。关于尖角关系可以分为两种情况，即主尖角关系和次尖角关系。一般来说当点源偏离尖角的时候，主尖角关系的值要大于次尖角关系的值。

与尖角奇点不同，在对应于折叠线的临界曲线上，雅克比矩阵在沿着临界曲线方向上的分量不等于0。当一个点源从外部穿进一条折叠线时，将会在对应的临界曲线上新增加两个像。这两个像的符号相反，其中临界曲线外侧的像为正像，里侧的像为倒像。

研究折叠线时也可以把费马势，在折叠线所对应的临界曲线上展开，忽略掉高阶项，然后通过费马势的一阶导数等于0，得到对应在折叠线附近的透镜方程为

$$\beta_1 \simeq a\theta_1^2, \tag{1.4}$$

$$\beta_2 \simeq b\theta_2. \tag{1.5}$$

其中a和b为常数。通过透镜方程可以解得，当一个点源无限地接近折叠线的内侧时，这两个像的放大倍数均为无穷大，这时这两个像的放大倍数满足一个关系[14, 47]

$$R_{\text{fold}} = \frac{\mu_{\text{A}} + \mu_{\text{B}}}{|\mu_{\text{A}}| + |\mu_{\text{B}}|} = 0, \tag{1.6}$$

其中A，B分别表示了这两个像，这个结果也不依赖于透镜模型。同样有些观点认为这个公式的分子也是为0[2, 114]，在本文的第二章我们将证明分子通常也不为0。由此也说明了折叠线关系是有正负符号的，当点源靠近主尖角时，折叠线关系一般为负值；当靠近次尖角时，折叠线关系一般为正值。

目前已经观测到的100多个多像系统中，四像系统占有很大的比例，因为这样的透镜一般对应了椭圆的面密度投影。关于这些类星体的各个像的位置，已经有很好的平滑的椭圆透镜模型可以重复出来。关于尖角型和折叠线型透镜模型，存在着我们前面提到的两种放大关系：尖角关系和折叠线关系。然而在实际的类星体多像现象中，很多观测到的各个像的流量并不满足这两种放大关系，有些情况甚至很大地偏离了这两个关系。这种观测与理论上的偏差被称为流量反常现象。[78]。关于流量反常现象还没有非常好的理论解释，最常见的就是研究次结构对各个像流量的影响。目前已经有一些这方面的数值模拟工作，可以比较好地解释流量反常现象[5, 16, 81, 123]。

对于四像透镜系统，像存在三种最主要的分类类型：尖角，折叠线和十字类型。大多数的研究工作主要是研究前两种类型的流量关系，以及有关于cusp relation和fold relation的流量反常现象。受到前两者的启发，我们将在文章的第三章着重研究爱因斯坦十字类型，并定义一个新的统计量：cross relation。

快速射电暴（fast radio burst，FRB）是近些年非常热门研究领域，由Lorimer等人[71]在2007年首次探测到。快速射电暴是指遥远宇宙中突然出现的短暂而猛烈的无线电波暴发，持续时间极短，通常只有几毫秒，却能够释放出相当于太阳在一整天内释放的能量。目前已经探测到的爆发仅有20余例[2]，大多是由Parkes[75]射电望远镜观测到的。虽然目前关于快速射电暴的物理起源尚不清楚，但是它们绝大多数爆发于高银纬处，而且它们的色散量要远远超过银河系星际介质的贡献，因此一般认为它们是河外起源甚至是宇宙学起源。目前对于FRB 的形成机制还不清楚，尤其在观测到的FRB中存在部分的双峰FRB，更是很难解释其形成原因。

2016年，Muñoz等人[83]首次提出MACHOs天体或者原初黑洞（PBH），可能是造成FRB双峰形成的原因。位于加拿大的在建的射电望远镜CHIME[11]，预计每年可以观测到10000个FRB。如果在$20--100\,M_{\odot}$的质量窗口，MACHOs天体组成了宇宙中全部的暗物质，我们将会观测到数十至数百个双峰结构每年。如果在这10000个FRB 中，没有观测到任何的双峰结构，我们则可以限制在质量$M_{\rm L} > 20\,M_{\odot}$窗口MACHOs中暗物质占所有暗物质的比例$f_{\rm DM}$为$f_{\rm DM} < 0.08$。在本论文中，我们将基于FRB双峰的引力透镜机制，进一步的探讨基于观测到的双峰对透镜体黑洞质量等性质的研究。

[2]http://astronomy.swin.edu.au/pulsar/frbcat/

第二章　Cusp Summations and Cusp Relations of Simple Quad Lenses

2.1 Introduction

Producing multiple images of distant quasars or galaxies by foreground galaxies or galaxy clusters is one of the most distinct qualities of strong gravitational lensing. For nonsingular lenses, it is well known that the total image number is odd [18]. If a point source lies within the central astroid caustic of the elliptic lens, there will be five images produced. There are two positive minima (minima point of Fermat potential, similar hereafter) images outside of the tangential critical curve, two negative saddle images inside of the tangential critical curve, and one positive maxima image lying near the lens centre [14, 98]. However, the maxima image located near the lens centre is usually highly demagnified and faint, resulting in four observed images.

There are some important magnification relations for the multiple image lenses. The magnification invariant means that, for some specific lens models, the sum of signed magnifications for all lensed images of a given point source is a constant, i.e., $I = \sum_i \mu_i$ [34]. It is very interesting and surprising that the invariants are independent of most of the model parameters. For example, the magnification invariants of the point lens and Singular Isothermal Sphere (SIS) lens are 1 and 2 respectively, no matter how large the Einstein radii are and where the positions of the point sources are, as long as there are two images produced.

The cusp and fold relations are local magnification relations compared with the magnification invariant. If a point source moves to the cusp from the inner side of the tangential caustic, three of the images will merge together near the critical curve. The three close images have an asymptotic magnification relation [14, 76, 101, 102]

$$R_{\rm cusp} = \frac{S_{\rm cusp}}{S_{|\rm cusp|}} = \frac{\mu_{\rm A} + \mu_{\rm B} + \mu_{\rm C}}{|\mu_{\rm A}| + |\mu_{\rm B}| + |\mu_{\rm C}|}, \tag{2.1}$$

where μ are the signed magnifications of the triple images A, B and C. Here, we define $S_{\rm cusp}$ and $S_{|\rm cusp|}$, and name the numerator $S_{\rm cusp}$ *cusp summation*, which will be frequently used in this work. If the point source infinitely approaches the cusp, the cusp relation $R_{\rm cusp}$ will be close to 0.

A similar magnification relation holds when the source lies near a fold caustic. In this case, two images lie closely together, straddling the critical curve. One of two images is a minima and the other one is a saddle. The fold image pair also has an asymptotic magnification relation [14, 47, 60, 76, 102]

$$R_{\rm fold} = \frac{S_{\rm fold}}{S_{|\rm fold|}} = \frac{\mu_{\rm A} + \mu_{\rm B}}{|\mu_{\rm A}| + |\mu_{\rm B}|}, \tag{2.2}$$

where μ are the signed magnifications of the double images A and B. Here, we define $S_{\rm fold}$ *fold summation* and another quantity $S_{|\rm fold|}$ as before. If the source infinitely approaches the fold line, the fold relation $R_{\rm fold}$ will also be close to 0.

In some previous works, when the point source infinitely approaches the cusp or the fold, the numerators in Equations 2.1 and 2.2 are also considered to be equal to 0 [2, 92, 125]. In our recent work, we (Chu, Lin & Yang 28) proved that $S_{\rm cusp}$ and $S_{\rm fold}$ are usually not equal to 0. Consequently, there are different signs in the numerators, so in the definitions about the two relations we do not use the absolute value of the summed magnifications in the numerators as some other authors do.

In strong gravitational lensing, the positions of most multiple images can be fitted adequately using simple smooth lens models. Nevertheless, the observed flux ratios are more difficult to match [63]. Actually, most of the observed fluxes of image pairs and triples disagree with the fold and cusp relations. The discrepancy between the predicted and observed flux ratios is commonly referred to as the anomalous flux ratio problem [31, 78, 79, 104]. Currently the most favoured explanation of the flux ratio anomalies invokes the perturbation effects from small-scale structures hosted by lensing galaxies [1, 25, 65, 72, 77, 81, 123, 124]. In this work, based on the magnification invariant, we mainly study the cusp summation and cusp relation through five frequently used smooth quad lenses, and they may be helpful for our understanding of the anomalous flux ratio problem in another aspect.

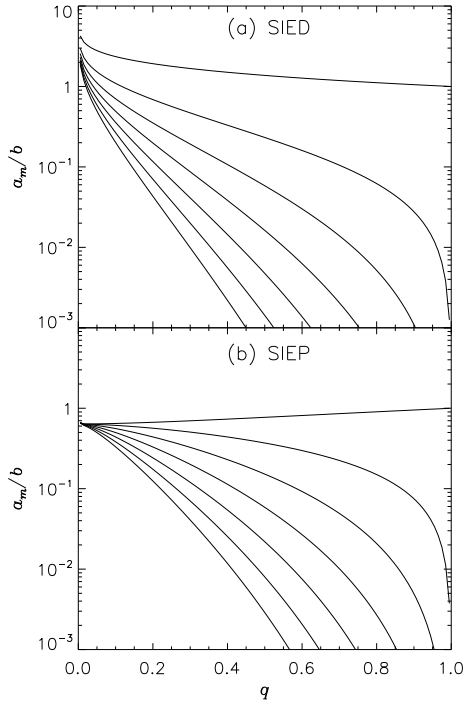

图 2.1: The coefficients of multipole expansions of the SIED and SIEP lenses. For each panel, the seven curves describe the coefficients of modes $m = 0$, 2, 4, 6, 8, 10, 12 from top to bottom, respectively.

2.2 General Review for the Five Quad Lenses

We review five often used quad lenses in strong lensing, including Singular Isothermal Elliptical Density (SIED), Singular Isothermal Elliptical Potential (SIEP), Singular Isothermal Quadrupole (SIQ), SIS+shear, and Point+shear lenses. There are some similar properties for the five lenses. For each lens model, the radial critical curve degenerates into a point in the lens centre, and corresponds to the pseudo-caustic [37]. Each of the five lenses has an astroid caustic which has four cusps and four folds, and each lens can produce four images at most for a single source.

The detailed information about these lenses is shown in Table 2.2. Each lens model has two parameters, including one that describes the intensity of non-dimensional mass density, and the other one that describes the deviation from

表 2.1: Five simple quad lenses.

Lens model	SIED[a] (x, y)	SIEP[b] (x, y)
Parameters	$b,\ q\ (0 < q < 1)$	$b,\ q\ (0 < q \leqslant 1)$
Convergence	$\kappa = \frac{b}{2\sqrt{q^2x^2+y^2}}$	$\kappa = \frac{bq^2(x^2+y^2)}{2(q^2x^2+y^2)^{3/2}}$
Deflection potential	$\psi = x\alpha_x + y\alpha_y$	$\psi = b\sqrt{q^2x^2+y^2}$
Deflection angle	$\alpha_x = \frac{b}{\sqrt{1-q^2}} \tan^{-1}\left(\sqrt{\frac{1-q^2}{q^2x^2+y^2}}x\right)$	$\alpha_x = \frac{bq^2x}{\sqrt{q^2x^2+y^2}}$
Deflection angle	$\alpha_y = \frac{b}{\sqrt{1-q^2}} \tanh^{-1}\left(\sqrt{\frac{1-q^2}{q^2x^2+y^2}}y\right)$	$\alpha_y = \frac{by}{\sqrt{q^2x^2+y^2}}$
Shear	$\gamma = \kappa$	$\gamma = \kappa$
Magnification	$\mu^{-1} = 1 - 2\kappa$	$\mu^{-1} = 1 - 2\kappa$
Critical curve	$q^2x^2 + y^2 = b^2$	$\frac{bq^2(x^2+y^2)}{(q^2x^2+y^2)^{3/2}} = 1$
Major axis $\beta_{\rm cusp}$	$\frac{b}{q} - \frac{b}{\sqrt{1-q^2}} \tan^{-1}\left(\frac{\sqrt{1-q^2}}{q}\right)$	$\frac{b}{q} - bq$
Minor axis $\beta_{\rm cusp}$	$-b + \frac{b}{\sqrt{1-q^2}} \tanh^{-1}(\sqrt{1-q^2})$	$b - bq^2$
Naked cusp	$q \lesssim 0.39$	$q < \sqrt{2}/2$
Magnification invariant[f]	≈ 2.8	2

the circular lens. For the two SIE lenses, they are usually studied in the Cartesian coordinates, while for the last three lens models, it is more convenient to treat them in polar coordinates.

The two SIE lenses are extended from the SIS lens. Here b is used as a constant parameter, which indicates the intensity of the mass density. q is the axial ratio of the SIE lens. The SIE lenses can be derived by changing θ into $\sqrt{q^2x^2+y^2}$ through the SIS lens. For the SIED lens the θ was changed in the mass distribution κ, while for the SIEP lens it was changed in the potential ψ.

For the SIED and SIEP lenses, their convergence can also be written in the form of polar coordinates

$$\kappa_{\rm SIED} = \frac{1}{2\theta}\frac{b}{\sqrt{q^2\cos^2\phi + \sin^2\phi}} = \frac{1}{2\theta}\frac{b\sqrt{1+\epsilon}}{\sqrt{1-\epsilon\cos 2\phi}}, \tag{2.3}$$

$$\kappa_{\rm SIEP} = \frac{1}{2\theta}\frac{bq^2}{(q^2\cos^2\phi + \sin^2\phi)^{3/2}} = \frac{1}{2\theta}\frac{b\sqrt{1+\epsilon}(1-\epsilon)}{(1-\epsilon\cos 2\phi)^{3/2}}. \tag{2.4}$$

Here, the parameter ϵ is related to the axial ratio q by $\epsilon = (1-q^2)/(1+q^2)$.

For each SIE lens, the convergence has the form $\kappa = G_{\rm SIE}(\phi)/2\theta$. The shape function $G_{\rm SIE}(\phi)$ can be decomposed into multipoles through Fourier transform

SIQ[c] (θ,ϕ)	SIS+shear[d] (θ,ϕ)	Point+shear[e] (θ,ϕ)
$\theta_{\rm E},\ k\ (0\leqslant k\leqslant 1)$	$\theta_{\rm E},\ \gamma\ (0\leqslant\gamma<1)$	$\theta_{\rm E},\ \gamma\ (0\leqslant\gamma<1)$
$\kappa=\frac{\theta_{\rm E}}{2\theta}(1+k\cos 2\phi)$	$\kappa=\frac{\theta_{\rm E}}{2\theta}$	$\kappa=\pi\theta_{\rm E}^2\delta(\boldsymbol{\theta})$
$\psi=\theta_{\rm E}\theta-\frac{1}{3}\theta_{\rm E}k\theta\cos 2\phi$	$\psi=\theta_{\rm E}\theta-\frac{\gamma}{2}\theta^2\cos 2\phi$	$\psi=\theta_{\rm E}^2\ln\theta-\frac{\gamma}{2}\theta^2\cos 2\phi$
$\alpha_{\rm rad}=\theta_{\rm E}-\frac{1}{3}\theta_{\rm E}k\cos 2\phi$	$\alpha_{\rm rad}=\theta_{\rm E}-\gamma\theta\cos 2\phi$	$\alpha_{\rm rad}=\frac{\theta_{\rm E}^2}{\theta}-\gamma\theta\cos 2\phi$
$\alpha_{\tan}=\frac{2}{3}\theta_{\rm E}k\sin 2\phi$	$\alpha_{\tan}=\gamma\theta\sin 2\phi$	$\alpha_{\tan}=\gamma\theta\sin 2\phi$
$\gamma=\kappa$	$\boldsymbol{\gamma}=\frac{\theta_{\rm E}}{2\theta}+\gamma\cos 2\phi-{\rm i}\gamma\sin 2\phi$	$\boldsymbol{\gamma}=\frac{\theta_{\rm E}^2}{\theta^2}+\gamma\cos 2\phi-{\rm i}\gamma\sin 2\phi$
$\mu^{-1}=1-2\kappa$	$\mu^{-1}=1-\gamma^2-\frac{\theta_{\rm E}}{\theta}(1+\gamma\cos 2\phi)$	$\mu^{-1}=1-\gamma^2-\frac{\theta_{\rm E}^4}{\theta^4}-2\frac{\theta_{\rm E}^2}{\theta^2}\gamma\cos 2\phi$
$\theta=\theta_{\rm E}+\theta_{\rm E}k\cos 2\phi$	$\theta=\theta_{\rm E}\frac{1+\gamma\cos 2\phi}{1-\gamma^2}$	$\left(\frac{\theta_{\rm E}}{\theta}\right)^2=\sqrt{1-\gamma^2\sin^2 2\phi}-\gamma\cos 2\phi$
$\frac{4}{3}\theta_{\rm E}k$	$2\theta_{\rm E}\frac{\gamma}{1-\gamma}$	$2\theta_{\rm E}\frac{\gamma}{\sqrt{1-\gamma}}$
$\frac{4}{3}\theta_{\rm E}k$	$2\theta_{\rm E}\frac{\gamma}{1+\gamma}$	$2\theta_{\rm E}\frac{\gamma}{\sqrt{1+\gamma}}$
$k>0.6$	$\gamma>1/3$	Never
1	$2/(1-\gamma^2)$	$1/(1-\gamma^2)$

[a]Kassiola & Kovner [55], Keeton & Kochanek [57], Keeton, Mao & Witt [58], Kormann, Schneider & Bartelmann [68]. [b]Kassiola & Kovner [55], Witt, Mao & Keeton [120]. [c]Chu, Lin & Yang [28], Kochanek [63], Woldesenbet & Williams [121]. [d]Finch et al. [44], Keeton, Gaudi & Petters [59], Kovner [69]. [e]An & Evans [6], Chang & Refsdal [22, 23], Schneider, Ehlers & Falco [102]. [f]Dalal [34], Dalal & Rabin [35], Witt & Mao [119]

method [59]

$$
\begin{aligned}
G_{\rm SIE}(\phi)&=\sum_{m=0}^{\infty}a_m\cos m\phi,\\
a_m&=\frac{1}{2\pi}\int_0^{2\pi}G_{\rm SIE}(\phi)\cos m\phi{\rm d}\phi.
\end{aligned}
\tag{2.5}
$$

Based on the symmetry of the SIE lenses, the coefficients a_m of the odd modes are equal to 0. Therefore, there are only even modes in the expansions, and their phases ϕ_m are all equal to 0.

Figure 2.1 shows the Fourier expansion coefficients of the shape functions of the SIE lenses. The strength of the monopole is the largest one among all modes. Since the Einstein radius is determined by the monopole, the Einstein radius of the SIE lens is $\theta_{\rm E}=a_0$. For a given parameter b, with increasing the ratio q, $\theta_{\rm E}$ decreases for the SIED lens, while increases for the SIEP lens. Except the monopole a_0, with increasing q, all the coefficients of the two SIE lenses decrease. In addition, the coefficients of all the even modes decrease with increasing of the mode m. The SIQ lens, also called SIS+elliptical lens [34, 121], can be thought

as the lowest order multipole expansion of the two SIE lenses, and its coefficients only include the monopole a_0 and the quadrupole a_2.

In polar coordinates, the shear can be decomposed into two parts, tangential or radial shear γ_+, and skew shear $\gamma_\times$ [12]. We can write them into the complex form $\boldsymbol{\gamma} = \gamma_+ + \mathrm{i}\gamma_\times$. The direction of the skew shear is rotated 45° from those of the tangential or radial shear. For the real part, when $\gamma_+ > 0$, it is tangential shear, while oppositely it is radial shear. The radial shear is only obvious for the void or the lens with negative mass distributions. For example, the convergence $\kappa = \cos 2\phi/2\theta$, can produce tangential shear in the positive density region, and radial shear in the negative region. In addition, the external shear γ in the last two lens models can bring both $\gamma_+ = \gamma\cos 2\phi$ and $\gamma_\times = -\gamma\sin 2\phi$ components.

For any lens with a convergence of the form of $G(\phi)/2\theta$, one can decompose it into multipoles, similar to Equation 2.5. For each mode of this lens, except $m = 1$, it has $\gamma = \kappa$ [27]. These shears are all tangential or radial ones γ_+, not including skew shear $\gamma_\times$. According to the superposition principle, we can conclude that, as long as the function $G(\phi)$ do not include the $m = 1$ mode, the shear of the lens is $\gamma = \kappa$, and the magnification is $\mu = 1/(1-2\kappa)$. In fact, Witt, Mao & Keeton [120] found that the lens potential with $\psi = \theta F(\phi)$ form has the magnification of $\mu = 1/(1-2\kappa)$. It is consistent with our conclusion, because for a convergence $G(\phi)/2\theta$ with no monopole, the lens potential can be written in the form $\psi = \theta F(\phi)$ [39, 40].

The last two lenses are derived by adding a uniform external shear on the SIS or the point lens. The point+shear lens is also called Chang-Refsdal lens [22, 23]. There is usually a minus sign before γ in few other studies. We use it in this form to let the major axis lie along the X-axis, and minor axis along the Y-axis. For a general strong lens, when the θ is infinite large, the magnification μ should have a positive sign. Therefore, it needs the external shear γ to be smaller than 1. However, it could also be studied with $\gamma > 1$ for extreme cases, as in An & Evans [6].

In addition, the convergence $\pi\theta_{\mathrm{E}}^2\delta(\boldsymbol{\theta})$ of the point lens or the point+shear lens is derived through the relation of the two-dimensional Dirac delta function